NASA/TM-2008-214641

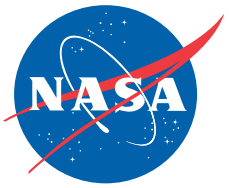

Nonlinear System Identification for Aeroelastic Systems with Application to Experimental Data

Dr. Sunil L. Kukreja
NASA Dryden Flight Research Center
Edwards, California

November 2008

NASA STI Program ... in Profile

Since its founding, NASA has been dedicated to the advancement of aeronautics and space science. The NASA scientific and technical information (STI) program plays a key part in helping NASA maintain this important role.

The NASA STI program is operated under the auspices of the Agency Chief Information Officer. It collects, organizes, provides for archiving, and disseminates NASA's STI. The NASA STI program provides access to the NASA Aeronautics and Space Database and its public interface, the NASA Technical Report Server, thus providing one of the largest collections of aeronautical and space science STI in the world. Results are published in both non-NASA channels and by NASA in the NASA STI Report Series, which includes the following report types:

- TECHNICAL PUBLICATION.
  Reports of completed research or a major significant phase of research that present the results of NASA programs and include extensive data or theoretical analysis. Includes compilations of significant scientific and technical data and information deemed to be of continuing reference value. NASA counterpart of peer-reviewed formal professional papers but has less stringent limitations on manuscript length and extent of graphic presentations.

- TECHNICAL MEMORANDUM.
  Scientific and technical findings that are preliminary or of specialized interest, e.g., quick release reports, working papers, and bibliographies that contain minimal annotation. Does not contain extensive analysis.

- CONTRACTOR REPORT.
  Scientific and technical findings by NASA-sponsored contractors and grantees.

- CONFERENCE PUBLICATION.
  Collected papers from scientific and technical conferences, symposia, seminars, or other meetings sponsored or cosponsored by NASA.

- SPECIAL PUBLICATION.
  Scientific, technical, or historical information from NASA programs, projects, and missions, often concerned with subjects having substantial public interest.

- TECHNICAL TRANSLATION.
  English-language translations of foreign scientific and technical material pertinent to NASA's mission.

Specialized services also include creating custom thesauri, building customized databases, and organizing and publishing research results.

For more information about the NASA STI program, see the following:

Access the NASA STI program home page at http://www.sti.nasa.gov

- E-mail your question via the Internet to help@sti.nasa.gov

- Fax your question to the NASA STI Help Desk at (301) 621-0134

- Phone the NASA STI Help Desk at (301) 621-0390

- Write to:
  NASA STI Help Desk
  NASA Center for AeroSpace Information
  7115 Standard Drive
  Hanover, MD 21076-1320

NASA/TM-2008-214641

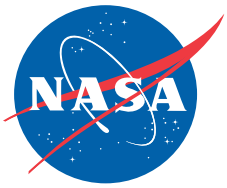

Nonlinear System Identification for Aeroelastic Systems with Application to Experimental Data

Dr. Sunil L. Kukreja
NASA Dryden Flight Research Center
Edwards, California

National Aeronautics and
Space Administration

Dryden Flight Research Center
Edwards, California 93523-0273

November 2008

Available from:

NASA Center for AeroSpace Information
7115 Standard Drive
Hanover, MD 21076-1320
(301) 621-0390

ABSTRACT

Representation and identification of a nonlinear aeroelastic pitch-plunge system as a model of the Nonlinear AutoRegressive, Moving Average eXogenous (NARMAX) class is considered. A nonlinear difference equation describing this aircraft model is derived theoretically and shown to be of the NARMAX form. Identification methods for NARMAX models are applied to aeroelastic dynamics and its properties demonstrated via continuous-time simulations of experimental conditions. Simulation results show that (1) the outputs of the NARMAX model closely match those generated using continuous-time methods, and (2) NARMAX identification methods applied to aeroelastic dynamics provide accurate discrete-time parameter estimates. Application of NARMAX identification to experimental pitch-plunge dynamics data gives a high percent fit for cross-validated data.

NOMENCLATURE

a	nondimensional distance from midchord to elastic axis
b	semichord of the wing
c_h	plunge structural damping coefficient
c_{l_α}	lift coefficient per angle of attack
c_{l_β}	lift coefficient per control surface deflection
c_{m_α}	moment coefficient per angle of attack
c_{m_β}	moment coefficient per control surface deflection
c_α	pitch structural damping coefficient
$e(n)$	uncontrolled input or innovation
ELS	extended least-squares
h	plunge motion
$\dot{h}$	plunge velocity
IV	instrumental variables
I_α	mass moment of inertia of the wing about the elastic axis
k_h	plunge structural spring constant
k_α	pitch structural spring constant
L	aerodynamic lift
LCO	limit cycle oscillations
LTI	linear time-invariant
m	wing mass
M	aerodynamic moment
ML	maximum likelihood
n	sampled data point index

n_e	maximum error lag
n_u	maximum input lag
n_z	maximum output lag
N	record length
N_v	validation record length
NARMAX	Nonlinear AutoRegressive, Moving Average eXogenous
PEI	prediction error identification
SNR	signal-to-noise ratio, dB
STD	standard deviation
T	sample time
u	controlled or exogenous input
U	free-stream velocity
WLS	weighted least-squares
x_α	nondimensional distance between elastic axis and center of mass
$y(n)$	output of the continuous time simulation
$\hat{y}(n)$	simulated output
z	measured output
%QF	percent quality of fit
f^l	nonlinear mapping
α	pitch angle
$\dot{\alpha}$	pitch velocity
$\ddot{\alpha}$	pitch acceleration
β	control surface deflection
$\delta(n)$	Kronecker impulse function
ρ	density of air

INTRODUCTION

System identification, or mathematical modeling, is the process of developing or improving a mathematical representation of a physical system based on observed data. System identification is a critical step in aircraft development, analysis, and validation for flight worthiness.

One such application of system identification in the flight-test community is for the analysis of aeroelasticity. The analysis of aeroelasticity is concerned with the interaction of inertial, structural, and aerodynamic forces (ref. 1). Previous approaches have modeled aeroelasticity with linear time-invariant (LTI) models. These linear models have

been successful in providing approximate estimates of an aircraft's response to gust, turbulence, and external excitations. However, when aircraft speeds increase to high subsonic or transonic Mach numbers, linear models no longer provide accurate predictions of the aircraft's behavior. Some of the behavior that cannot be modeled linearly includes transonic dip, airflow separation, and shock oscillations, which can induce nonlinear phenomena such as limit cycle oscillations (LCO) (refs. 2 and 3). The onset of LCOs has been observed on several aircraft, such as the F-16C (Lockheed Martin Corporation, Bethesda, Maryland) or F/A-18 (McDonnell Douglas Corporation, St. Louis, Missouri, now The Boeing Company, Chicago, Illinois), and cannot be modeled properly as an LTI system (ref. 4). This limitation has necessitated the application of nonlinear identification techniques to accurately model LCO dynamics.

Over the past several decades, significant achievements have been made in several areas of nonparametric nonlinear system identification (e.g., refs. 5–7). Recent work in the aerospace community has attempted to address these nonlinear aeroelastic phenomena using Volterra kernel methods (ref. 8). These methods provide a convenient means of characterizing LCOs but suffer from a highly over-parameterized model description and do not lend themselves to efficient control synthesis.

Parametric representations of nonlinear systems typically contain a small number of coefficients that can be varied to alter the behavior of the equation and may be linked to the underlying system. Leontaritis and Billings (refs. 9 and 10) have proposed the Nonlinear AutoRegressive, Moving Average eXogenous (NARMAX) structure as a general parametric form for modeling nonlinear systems. NARMAX models describe nonlinear systems in terms of linear-in-the-parameters difference equations relating the current output to (possibly nonlinear) combinations of inputs and past outputs. It is suitable for modeling both the stochastic and deterministic components of a system and is capable of describing a wide variety of nonlinear systems (refs. 11 and 12). This formulation yields compact model descriptions that may be readily identified and may afford greater interpretability. NARMAX models have been successfully demonstrated for modeling the input-output behavior of many complex systems such as ones found in engineering and biology (refs. 13 and 14).

Currently, development and test of aircraft takes many years and considerable expenditure of limited resources. One reason for lengthy development time and costs is that many models (and hence control strategies) need to be developed throughout the flight envelope. The power of parametric nonlinear identification techniques (i.e., NARMAX models) is that they can describe complex aeroelastic behavior over a large operating range. Consequently, models are provided that can be more robust and reduce development time.

Although the NARMAX structure is well-suited to modeling the input-output behavior of an aeroelastic system, this method has not been investigated by the flight-test community to date. Therefore, the objectives of this report are to (1) theoretically analyze a nonlinear pitch-plunge model of aircraft dynamics to derive its NARMAX representation,

(2) assess the applicability of this nonlinear model for the identification of aerospace systems, and (3) investigate the suitability of NARMAX identification methods applied to aircraft dynamics.

The results show that the NARMAX model class provides an ideal framework for modeling the input-output behavior of a nonlinear pitch-plunge model describing aircraft dynamics. Identification results illustrate that methods for identification of NARMAX models are well-suited for identifying aircraft dynamics. Analysis of experimental data using NARMAX identification techniques provides a parameter set that explains the input-output data well. Overall, this report contributes to the understanding of the use of parametric identification techniques for modeling of aerospace systems.

The organization of this report is as follows. The NARMAX model structure is described in the section titled "NARMAX Model." In the section titled "Nonlinear Pitch-Plunge Model of Aircraft Dynamics," a continuous-time representation of a nonlinear pitch-plunge model describing aircraft dynamics is given, while its NARMAX representation is derived in the section titled "Theoretical Analysis." The section titled "Validation of NARMAX Pitch-Plunge Model" illustrates the results of simulating this NARMAX representation of pitch-plunge dynamics. In the section titled "NARMAX Identification of Pitch-Plunge Model," the applicability of NARMAX identification to this model representation via simulations of experimental condition is assessed. The section titled "Identification of Experimental Pitch-Plunge Data" presents the results of identifying experimental wind tunnel data, and the "Discussion" section provides a discussion of the major finds. Lastly, conclusions and significance of the results are given in the "Conclusion" section.

NARMAX MODEL

The NARMAX structure is a general parametric form for modeling nonlinear systems (ref. 9). This structure describes both the stochastic and deterministic components of nonlinear systems. Many nonlinear systems are a special case of the general NARMAX structure (ref. 12). The NARMAX structure models the input-output relationship as a nonlinear difference equation of the form shown in equation (1):

$$z(n) = f^{l}\left[z(n-1),\cdots,z\left(n-n_z\right),u(n),\cdots,u\left(n-n_u\right),e(n-1),\cdots,e\left(n-n_e\right)\right]+e(n) \qquad (1)$$

f^{l} denotes a nonlinear mapping; u is the controlled or exogenous input; z is the measured output; and e is the uncontrolled input or innovation. The nonlinear mapping, f^{l}, can be described by a wide variety of nonlinear functions such as a tanh(·) or splines (i.e., hard nonlinearities) (refs. 11 and 12). For simplicity, nonlinearities are only considered that can be described by a polynomial expansion. This class of nonlinear difference equations describes the dynamic behavior of a system as a linear and/or nonlinear expansion of the input, output, and error. These equations may include a variety of nonlinear terms, such as terms raised to an integer power (e.g., $u^3(n-5)$); products of present and

past inputs (e.g., $u(n)u(n-3)$); past outputs (e.g., $z^2(n-2)z(n-7)$); or cross-terms (e.g., $u(n-3)z^2(n-4)$). This system description encompasses many forms of nonlinear difference equations that are linear-in-the-parameters. Thus, there are no problems with local minima.

NONLINEAR PITCH-PLUNGE MODEL OF AIRCRAFT DYNAMICS

O'Neil et al. (refs. 15 and 16) developed a nonlinear pitch-plunge model (fig. 1) describing aircraft aeroelastic dynamics. Figure 1 characterizes aeroelastic wing dynamics for experiments performed on the Texas A&M University (College Station, Texas) testbed (ref. 16). This model provides a relationship between control surface deflection as input, and pitch-plunge displacement and velocity as outputs, of a single-input multiple-output nonlinearity followed by a simple integrator.

The model presented in figure 1 has been derived from the governing equations of motion for aeroelastic systems, as shown in equation (2):

$$\begin{bmatrix} m & mx_\alpha b \\ mx_\alpha b & I_\alpha \end{bmatrix} \begin{bmatrix} \ddot{h} \\ \ddot{\alpha} \end{bmatrix} + \begin{bmatrix} c_h & 0 \\ 0 & c_\alpha \end{bmatrix} \begin{bmatrix} \dot{h} \\ \dot{\alpha} \end{bmatrix} + \begin{bmatrix} k_h & 0 \\ 0 & k_\alpha(\alpha) \end{bmatrix} \begin{bmatrix} h \\ \alpha \end{bmatrix} = \begin{bmatrix} -L \\ M \end{bmatrix} \quad (2)$$

where h denotes plunge motion; α is the pitch angle; x_α is the nondimensional distance between elastic axis and center of mass; m is the wing mass; I_α is the mass moment of inertia of the wing about the elastic axis; b is the semichord of the wing; c_h and c_α are the plunge and pitch structural damping coefficients, respectively; k_h and k_α are the plunge and pitch structural spring constants, respectively; and L and M are the aerodynamic lift and moment, respectively.

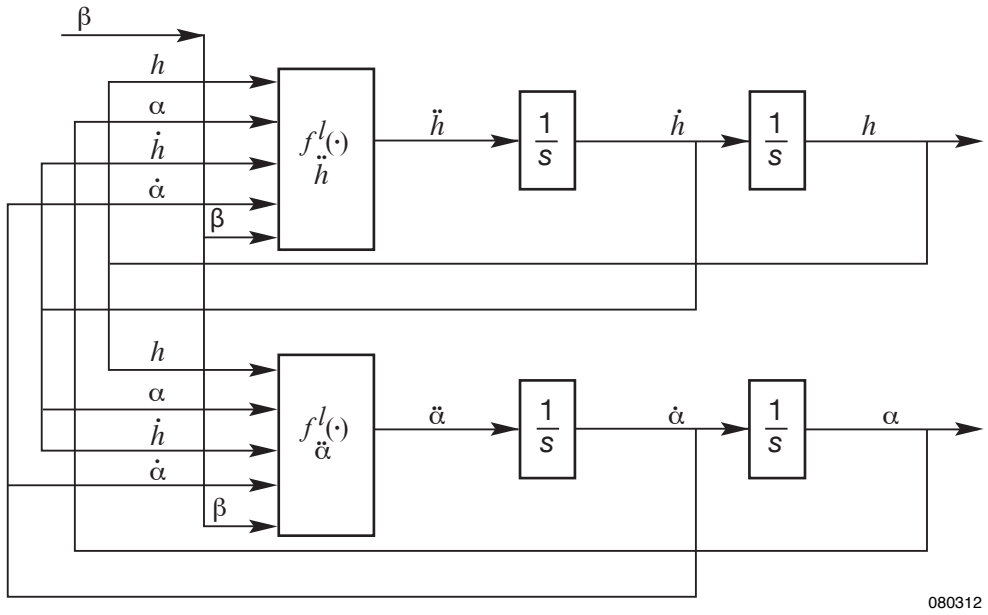

Figure 1. System structure assumed for modeling and identification of pitch-plunge aeroelastic dynamics.

Typically, quasi-steady aerodynamic forces and moments are assumed which can be modeled, as shown in equation (3):

$$\begin{aligned} L &= \rho U^2 b c_{l_\alpha}\left[\alpha + \frac{\dot{h}}{U} + \left(\frac{1}{2} - a\right) b\frac{\dot{\alpha}}{U}\right] + \rho U^2 b c_{l_\beta}\beta \\ M &= \rho U^2 b^2 c_{m_\alpha}\left[\alpha + \frac{\dot{h}}{U} + \left(\frac{1}{2} - a\right) b\frac{\dot{\alpha}}{U}\right] + \rho U^2 b^2 c_{m_\beta}\beta \end{aligned} \tag{3}$$

where ρ denotes density of air; U is the free-stream velocity; c_{m_α} and c_{l_α} are the moment and lift coefficients per angle of attack, respectively; c_{m_β} and c_{l_β} are the moment and lift coefficients per control surface deflection, respectively; β is the control surface deflection; and a is the nondimensional distance from midchord to elastic axis.

Although several classes of nonlinear mappings for stiffness contributions, $k_\alpha(\alpha)$, have been investigated for open loop dynamics of aeroelastic systems (refs. 17–20), the work of O'Neil et al. (refs. 15 and 16) demonstrated that a polynomial mapping of the form shown in equation (4) describes the behavior of this testbed well:

$$k_\alpha(\alpha) = k_{\alpha_0} + k_{\alpha_1}\alpha + k_{\alpha_2}\alpha^2 + k_{\alpha_3}\alpha^3 + k_{\alpha_4}\alpha^4 \tag{4}$$

Equations of motion are derived by combining equations (2) and (3) to yield equation (5):

$$\begin{bmatrix} m & mx_\alpha b \\ mx_\alpha b & I_\alpha \end{bmatrix}\begin{bmatrix} \ddot{h} \\ \ddot{\alpha} \end{bmatrix}+\begin{bmatrix} c_h+\rho Ubc_{l_\alpha} & \rho Ub^2c_{l_\alpha}\left(\frac{1}{2}-a\right) \\ \rho Ub^2c_{m_\alpha} & c_\alpha-\rho Ub^3c_{m_\alpha}\left(\frac{1}{2}-a\right) \end{bmatrix}\begin{bmatrix} \dot{h} \\ \dot{\alpha} \end{bmatrix}$$
$$+\begin{bmatrix} k_h & \rho U^2bc_{l_\alpha} \\ 0 & -\rho U^2b^2c_{m_\alpha}+k_\alpha(\alpha) \end{bmatrix}\begin{bmatrix} h \\ \alpha \end{bmatrix}=\begin{bmatrix} -\rho bc_{l_\beta} \\ \rho b^2c_{m_\beta} \end{bmatrix}U^2\beta \tag{5}$$

The model form presented in figure 1 is derived by transforming equation (5) to give equation (6):

$$\dot{\mathbf{x}}=\mathbf{f}_\mu(\mathbf{x})+\mathbf{g}(\mathbf{x})\mu\beta \tag{6}$$

where $\mathbf{x}=\begin{bmatrix} x_1 & x_2 & x_3 & x_4 \end{bmatrix}^T=\begin{bmatrix} h & \alpha & \dot{h} & \dot{\alpha} \end{bmatrix}^T$; $\mu=U^2$; and $\mathbf{f}_\mu$ and $\mathbf{g}(\mathbf{x})$ are as given in equation (7):

$$\mathbf{f}_\mu=\begin{bmatrix} x_3 \\ x_4 \\ -k_1x_1-\left(k_2\mu+p\left(x_2\right)\right)x_2-c_1x_3-c_2x_4 \\ -k_3x_1-\left(k_4\mu+q\left(x_2\right)\right)x_2-c_3x_3-c_4x_4 \end{bmatrix},\mathbf{g}(\mathbf{x})=\begin{bmatrix} 0 \\ 0 \\ g_3 \\ g_4 \end{bmatrix} \tag{7}$$

The supplementary variables k_i, $i=1, 2, 3, 4$, and g_j, $j=3, 4$, are provided in table 1 in relationship to the aeroelastic parameters given in equations (2) and (3).

Table 1. Supplementary system variables.

Supplementary variable	Relationship to system parameters
d	$m\left(I_\alpha - mx_\alpha^2 b^2\right)$
k_1	$\frac{I_\alpha k_h}{d}$
k_2	$\frac{I_\alpha \rho b c_{l_\alpha} + mx_\alpha b^3 \rho c_{m_\alpha}}{d}$
k_3	$\frac{-mx_\alpha b k_h}{d}$
k_4	$\frac{-mx_\alpha b^2 \rho c_{l_\alpha} - m\rho b^2 c_{m_\alpha}}{d}$
c_1	$\frac{I_\alpha\left(c_h + \rho U b c_{l_\alpha}\right) + mx_\alpha \rho U b^3 c_{m_\alpha}}{d}$
c_2	$\frac{I_\alpha \rho U b^2 c_{l_\alpha}\left(\frac{1}{2} - a\right) - mx_\alpha b c_\alpha + mx_\alpha \rho U b^4 c_{m_\alpha}\left(\frac{1}{2} - a\right)}{d}$
c_3	$\frac{-mx_\alpha b c_h - mx_\alpha \rho U b^2 c_{l_\alpha} - m\rho U b^2 c_{m_\alpha}}{d}$
c_4	$\frac{mc_\alpha - mx_\alpha \rho U b^3 c_{l_\alpha}\left(\frac{1}{2} - a\right) - m\rho U b^3 c_{m_\alpha}\left(\frac{1}{2} - a\right)}{d}$
g_3	$\frac{-I_\alpha \rho b c_{l_\beta} - mx_\alpha b^3 \rho c_{m_\beta}}{d}$
g_4	$\frac{mx_\alpha b^2 \rho c_{l_\beta} + m\rho b^2 c_{m_\beta}}{d}$
$p\left(x_2\right)$	$\frac{-mx_\alpha b}{d} k_\alpha\left(x_2\right)$
$q\left(x_2\right)$	$\frac{m}{d} k_\alpha\left(x_2\right)$

Transformation of equation (5) to equation (6) and introduction of supplementary variables (table 1) provides the simple model description presented in figure 1. The nonlinear mappings for this model description are given as equations (8) and (9):

$$\begin{aligned} f^{l}_{\ddot{a}}(\cdot) &= -k_3 h(n)\left[k_4 \mu \frac{m}{d}\left(k_{\alpha_0} + k_{\alpha_1}\alpha + k_{\alpha_2}\alpha^2 + k_{\alpha_3}\alpha^3 + k_{\alpha_4}\alpha^4 \right) \right] \alpha(n) - c_3 \dot{h}(n) \\ &\quad - c_4 \dot{\alpha}(n) + g_4 \mu U(n) \\ &= -b_1 h(n) - \left[b_2 \alpha(n) + b_3 \alpha^2(n) + b_4 \alpha^3(n) + b_5 \alpha^4(n) + b_6 \alpha^5(n) \right] - b_7 \dot{h}(n) \\ &\quad - b_8 \dot{\alpha}(n) + b_9 U(n) \\ &= \ddot{\alpha}(n) \end{aligned} \tag{8}$$

$$\begin{aligned} f^{l}_{\ddot{h}}(\cdot) &= -k_1 h(n) - \left[k_2 \mu + \frac{-m x_\alpha b}{d}\left(k_{\alpha_0} + k_{\alpha_1}\alpha + k_{\alpha_2}\alpha^2 + k_{\alpha_3}\alpha^3 + k_{\alpha_4}\alpha^4 \right) \right] \alpha(n) \\ &\quad - c_1 \dot{h}(n) - c_2 \dot{\alpha}(n) + g_3 \mu U(n) \\ &= -a_1 h(n) - \left[a_2 \alpha(n) + a_3 \alpha^2(n) + a_4 \alpha^3(n) + a_5 \alpha^4(n) + a_6 \alpha^5(n) \right] - a_7 \dot{h}(n) \\ &\quad - a_8 \dot{\alpha}(n) + a_9 U(n) \\ &= \ddot{h}(n) \end{aligned} \tag{9}$$

Note that this system (fig. 1) can be described in terms of pitch-plunge displacement or velocity. Here, pitch-plunge is chosen in terms of velocity because (1) it offers a model description with lower dynamic order, and (2) velocity feedback models are often used for vibration suppression.

Discrete-Domain Approximations

Many methods exist for discretization of continuous-time systems and signals. Most commonly used are Euler's forward, Euler's backward, or Tustin's method (also known as the bilinear transformation method) (refs. 21 and 22). Each has its advantages as well as disadvantages. While Tustin's and Euler's backward methods provide a superior approximation to a continuous-time signal, the goal in system identification is not (directly) signal reproduction but model estimation.

Tustin's method provides excellent signal estimation, but its use for modeling a pure integrator yields system descriptions that can be overly complex (e.g., redundant terms). Euler's backward method also provides good signal estimation but provides a model that is not intuitive. Models based on this approximation would include the current output as one of the model terms, leading to an algebraic loop. Although Euler's forward method is well-known to be unstable, this is only true if the sampling rate is not sufficiently large.

For identification purposes this does not pose a concern since the signals need to be sampled *at least* twice Nyquist and, hence, stability is achieved. Generally, the rule of thumb is to sample a signal at least 4 to 10 times the highest known (or suspected) system dynamics (ref. 23). For the pitch-plunge system under investigation, Euler's forward method provides a model description that is both stable and intuitive. Moreover, all three methods converge to similar accuracies for sufficiently large sampling rates. For these reasons Euler's forward method is chosen to model the system dynamics.

THEORETICAL ANALYSIS

The pitch-plunge model is given in continuous-time. This section shows how the model can be converted to discrete-time and rewritten as a NARMAX model. To do so, note that the two nonlinearities can be decoupled and analyzed separately since they yield two separate model descriptions for pitch and plunge velocity.

Euler's forward (explicit) method (ref. 21), as shown in equation (10)

$$\frac{1}{s} = \dot{x}(0) + \int_0^t \ddot{x}(t)\,dt \approx \dot{x}(n-1) + T\ddot{x}(n-1) \tag{10}$$

where T is the sample time, was used to approximate the continuous-time integrator, where $\ddot{x}$ is replaced by $\ddot{\alpha}$ and $\ddot{h}$ for pitch and plunge, respectively.

The nonlinearities used for this analysis, to derive an input-output model of pitch and plunge, were given in equations (8) and (9). In addition, the models are assumed corrupted by output additive (measurement) noise, as shown in equation (11):

$$\begin{aligned} \dot{\alpha}(n) &= \dot{\alpha}_{nf}(n) + e_{\dot{\alpha}}(n) \\ \dot{h}(n) &= \dot{h}_{nf}(n) + e_{\dot{h}}(n) \end{aligned} \tag{11}$$

where $\dot{\alpha}(n)$ and $\dot{h}(n)$ are the noise-corrupted outputs, $\dot{\alpha}_{nf}(n)$ and $\dot{h}_{nf}(n)$ are the unmeasured noise-free outputs, and $e_{\dot{\alpha}}(n)$ and $e_{\dot{h}}(n)$ are the measurement noise.

After collecting and combining terms, the overall nonlinear models were represented as nonlinear difference equations with 10 terms each, as shown in equation (12):

$$
\begin{aligned}
\dot{\alpha}(n) &= \gamma_1\dot{\alpha}(n-1) + \gamma_2 h(n-1) + \gamma_3\alpha(n-1) + \gamma_4\alpha(n-1)^2 + \gamma_5\alpha(n-1)^3 \\
&\quad + \gamma_6\alpha(n-1)^4 + \gamma_7\alpha(n-1)^5 + \gamma_8\dot{h}(n-1) + \gamma_9 u(n-1) + \gamma_{10} e_{\dot{\alpha}}(n-1) + e_{\dot{\alpha}}(n) \\
\dot{h}(n) &= \theta_1\dot{h}(n-1) + \theta_2 h(n-1) + \theta_3\alpha(n-1) + \theta_4\alpha(n-1)^2 + \theta_5\alpha(n-1)^3 \\
&\quad + \theta_6\alpha(n-1)^4 + \theta_7\alpha(n-1)^5 + \theta_8\dot{\alpha}(n-1) + \theta_9 u(n-1) + \theta_{10} e_{\dot{h}}(n-1) + e_{\dot{h}}(n)
\end{aligned}
\tag{12}
$$

These are NARMAX models since they (1) include input-output terms that are combinations of linear and nonlinear integer powers and (2) are linear-in-the-parameters. Table 2 shows the relationship of discrete-time NARMAX parameters in equation (12) to the underlying continuous-time coefficients.

Table 2. Theoretical relationship of NARMAX model parameter set to continuous-time system coefficients.

NARMAX plunge coefficient	Relationship to continuous-time coefficient	NARMAX pitch coefficient	Relationship to continuous-time coefficient
θ_1	$1 - Ta_7$	γ_1	$1 - Tb_8$
θ_2	Ta_1	γ_2	Tb_1
θ_3	Ta_2	γ_3	Tb_2
θ_4	Ta_3	γ_4	Tb_3
θ_5	Ta_4	γ_5	Tb_4
θ_6	Ta_5	γ_6	Tb_5
θ_7	Ta_6	γ_7	Tb_6
θ_8	Ta_8	γ_8	Tb_7
θ_9	Ta_9	γ_9	Tb_9
θ_{10}	$-\left(1 - Ta_7\right)$	γ_{10}	$-\left(1 - Tb_8\right)$

VALIDATION OF NARMAX PITCH-PLUNGE MODEL

The accuracy of this system representation was validated by simulating the pitch-plunge model in continuous-time using Simulink® (The MathWorks, Natick, Massachusetts) (fig. 1). The nonlinearities used in this continuous-time simulation were the fifth-order power series described in equations (8) and (9). The parameters used in the simulation were typical values found in experiments and are given in table 3 (ref. 15). The system was excited using a 5-Hz chirp input.

Table 3. Continuous-time system coefficients.

CT coefficient	Value
b	0.135 m
span	0.600 m
k_h	2844.4 N/m
c_h	27.43 N s/m
ρ	1,225 kg/m^3
c_{l_α}	6.28/rad
c_{l_β}	3.358/rad
c_{m_α}	$(0.5 + a)c_{l_\alpha}$ / rad
c_{m_β}	-0.635/rad

Output Accuracy

To determine the validity of this NARMAX description model provided in equation (12), its response is simulated for a parameter set corresponding to those used for the continuous-time model. The input sequence was a 5-Hz chirp with a signal duration of 30 s. The chirp input had an operating range between ±1.0 rad, as shown in figure 2(a).

Using a fifth-order nonlinearity, the frequency content of the signal at the output of the nonlinearity will be at least 25 Hz (5 times the 5-Hz chirp signal). To avoid internal aliasing, a sampling rate of 100 Hz ($T = 0.01$ s) is selected, which is 4 times greater than the internal 25-Hz signal.

The simulated output, $\hat{y}(n)$, of the NARMAX description model was compared with the output of the continuous-time simulation, $y(n)$, by computing the percent variance accounted for by the NARMAX model as the percent quality of fit (%QF) provided in equation (13):

$$\%\mathrm{QF} = \left(1 - \frac{\frac{1}{N}\sum_{n=1}^{N}(y(n) - \hat{y}(n))^2}{\frac{1}{N}\sum_{n=1}^{N}(y(n))^2} \right) \times 100 \tag{13}$$

where N is the record length.

Simulation Result

The results of simulating the pitch-plunge model in continuous-time against the discrete-time NARMAX predictions are provided in figure 2. Figure 2 shows the simulation input (fig. 2(a)) and predicted velocity outputs of the NARMAX description models superimposed on top of the continuous-time outputs of the pitch (fig. 2(b)) and plunge (fig. 2(c)) velocity models. With over 99 %QF, the NARMAX outputs matched that of the continuous-time simulation with negligible error.

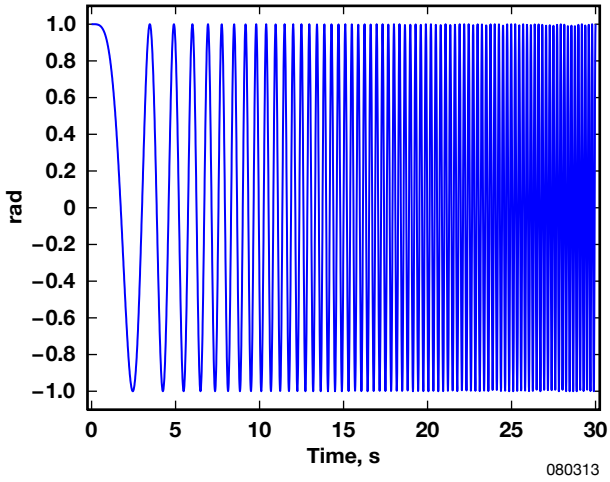

(a). Control surface deflection.

Figure 2. (a). Input to simulated pitch-plunge model in continuous-time and NARMAX description model; (b) and (c). Output of simulated pitch-plunge velocity model in continuous-time and NARMAX description model. Note that the two outputs are almost identical.

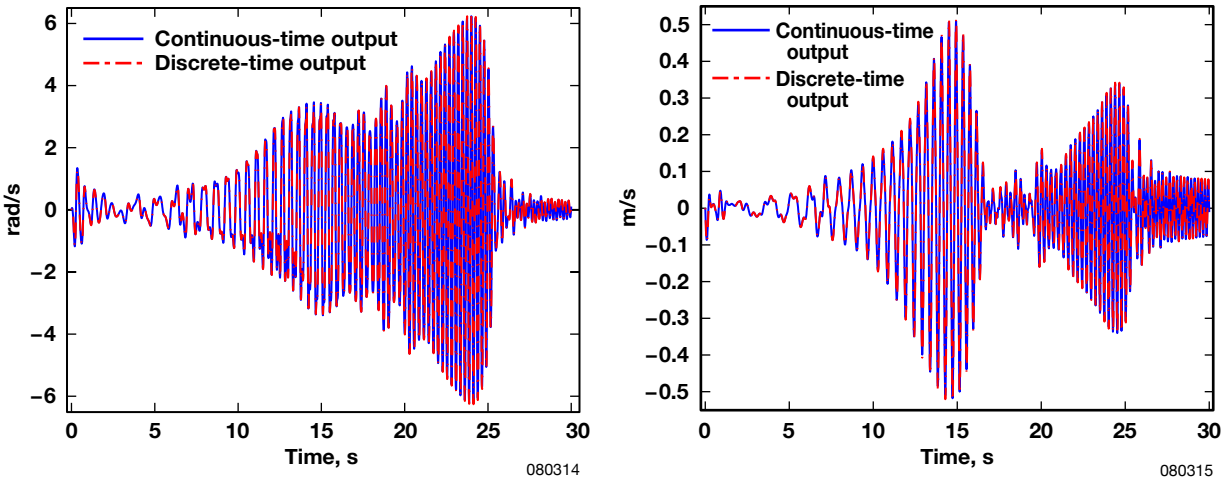

(b). Pitch velocity.

(c). Plunge velocity.

Figure 2. Concluded.

NARMAX IDENTIFICATION OF PITCH-PLUNGE MODEL

The utility of methods developed for identifying NARMAX models using sampled data from this continuous-time simulation were then assessed. An extended least-squares (ELS) algorithm (refs. 24–26) was used to identify model parameters.

The NARMAX description of the pitch-plunge velocity models (eq. (12)) is described by past outputs that are linear-in-the-parameters. In the presence of output additive noise (eqs. (11) and (12)), these terms result in lagged values of disturbance terms that are also *linear-in-the-parameters*. If these lagged errors are not modeled, they induce a bias in the parameter estimates (refs. 22, 27, and 28). The ELS algorithm was implemented because it is designed to model lagged-error terms thereby providing unbiased parameter estimates.

The fact that ELS may suffer from convergence problems (refs. 22, 29, and 30) is well-known. However, no prediction error identification (PEI) method is optimal. For the pitch-plunge velocity models, ELS is deemed the best estimation technique because it provides an unbiased estimate of model parameters (ref. 22). Other estimation techniques such as maximum likelihood (ML), instrumental variables (IV), weighted least-squares (WLS), etc., are difficult to implement and also have convergence problems (refs. 22, 30, and 31). For this reason ELS is chosen.

Analysis of NARMAX Model Parameters

A Monte Carlo study of these NARMAX parameters (eq. (12) and table 2) was performed to assess their accuracy and variability using the ELS estimator. One thousand Monte Carlo simulations were generated in which the input-output realization was the same but had a unique Gaussian, white, zero-mean, noise sequence added to the output. The output additive noise amplitude was increased in increments of 5 dB, from 20 to 0 dB signal-to-noise ratio (SNR). Parameter mean and standard deviation was computed from the 1000 estimates. The input used for this study was the same 5-Hz chirp signal previously described in the section titled “Output Accuracy.”

For this study, the system order and structure were assumed to be known with the coefficient set in equation (12) and tables 2 and 3. The regressor matrix used by this algorithm was formed to contain only those columns (parameters) that corresponded to the theoretical analysis (eq. (12)). A reasonable assumption is made that the order and structure are known because the goal is to identify a model in the model class described by equation (12).

In experimental settings, often only pitch-plunge displacement and/or acceleration signals are available. For a velocity model description, the velocity signal is required for identification. Therefore, pitch-plunge acceleration signals are numerically integrated to obtain a velocity profile. The estimation set consisted of $N = 3000$ data points sampled at $T = 0.01$ s. The estimated parameters were cross-validated with a fresh noise-corrupted output to compute the %QF of the predicted pitch and plunge velocity. The validation set consisted of $N_v = 3000$ data points (refs. 22 and 32).

Identification Results of Simulated Model

Figure 3 shows the results of identifying this simulated model of pitch-plunge. The NARMAX parameters in this figure correspond to those given in table 2. This figure shows that the identified parameter values corresponded closely to those derived theoretically for all SNRs. Note that the mean value of parameters γ_{10} and θ_{10} is not expected to be close to the theoretically computed value since they correspond to lagged-error terms. Lagged-error terms are difficult to identify accurately, even with high SNR, since the terms model the output additive noise, which is an unmeasurable stochastic process. This stochastic process is modeled (approximated) by a deterministic signal of prediction errors, which is only an (poor) estimate of the noise (refs. 22 and 28).

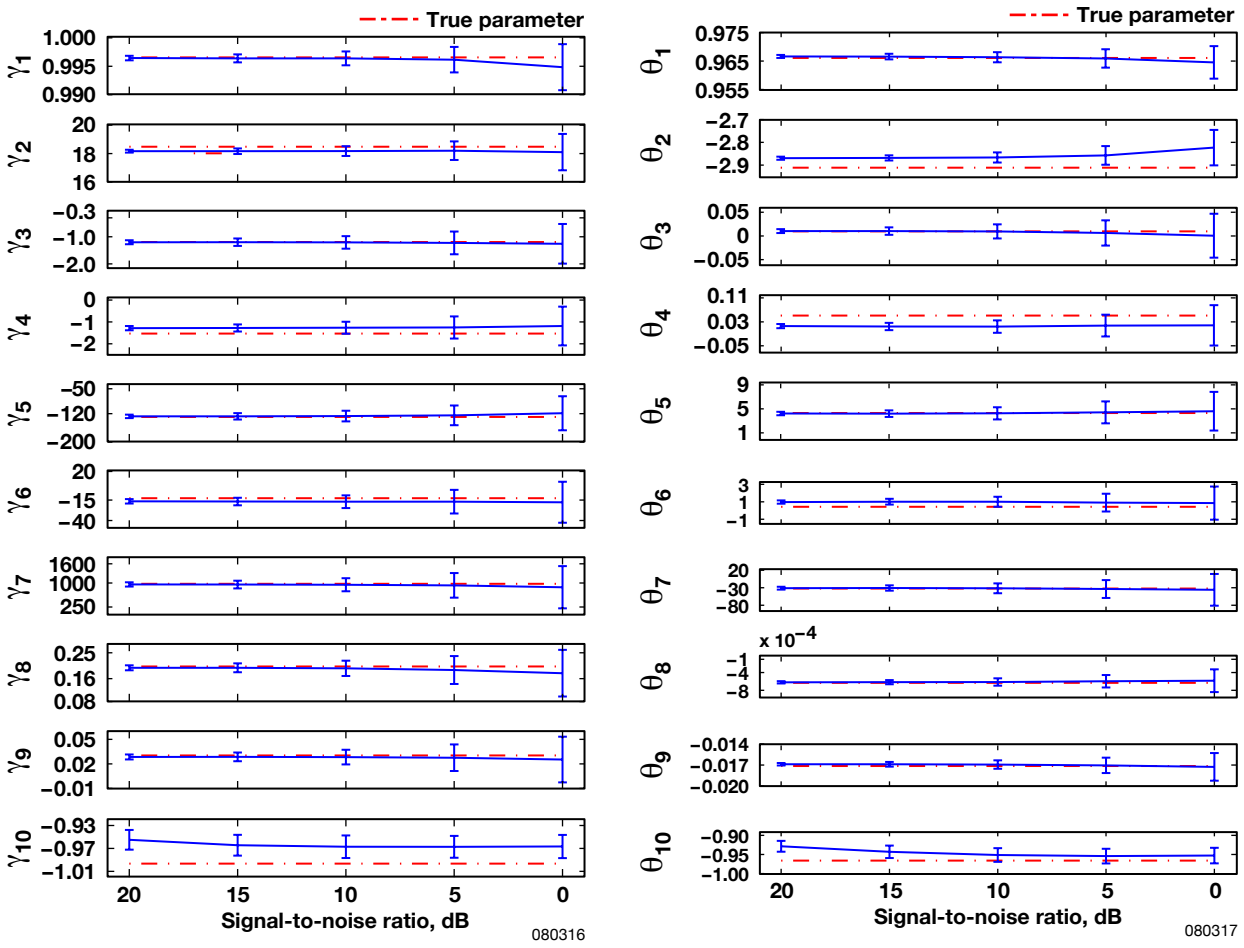

(a). Pitch parameters, mean and STD.

(b). Plunge parameters, mean and STD.

Figure 3. Monte Carlo study of pitch-plunge NARMAX model parameters. 5-Hz chirp input, Gaussian, white, zero-mean noise and $N = 3000$. Ordinate: STD about mean. Abscissa: Output SNR = 20, 15, 10, 5 and 0 dB. (Note that the abscissa is shown in decreasing SNR, which corresponds to increasing noise intensity.)

Figure 4 presents a result of cross-validation for a typical parameter set for this study. Figures 4(a) and 4(b) show a noise-corrupted output used for identification, and figures 4(c) and 4(d) show a predicted output superimposed on top of the noise-free output. The predicted output matched the measured output with over 98 %QF.

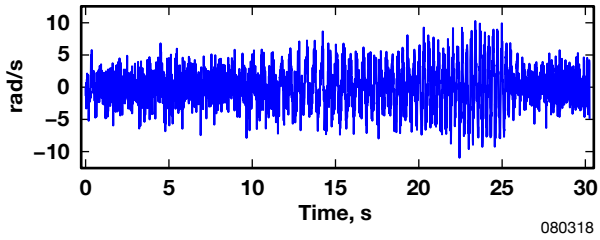

(a). Sampled continuous-time pitch velocity (noise corrupted 0 dB).

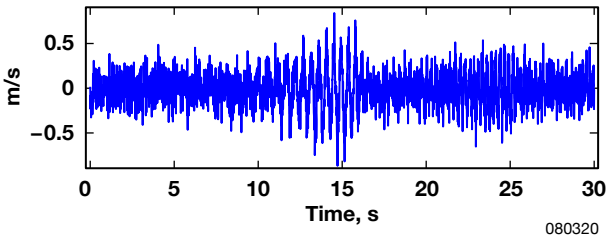

(b). Sampled continuous-time plunge velocity (noise corrupted 0 dB).

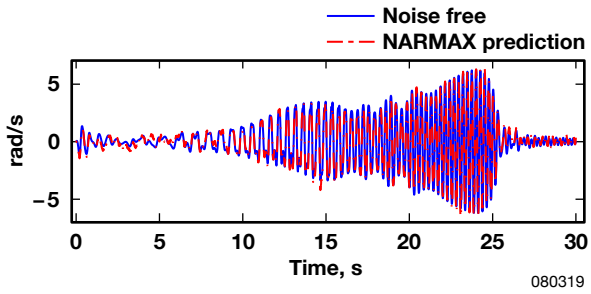

(c). Predicted pitch velocity: QF = 98.33%.

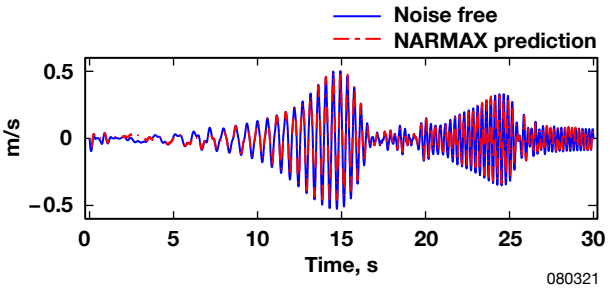

(d). Predicted plunge velocity: QF = 98.54%.

Figure 4. Cross-validation for typical identified NARMAX pitch (left) and plunge (right) models with N_v = 3000 and Gaussian, white, zero-mean output additive noise (0 dB SNR). Top panels: Measured outputs used for estimation. Bottom panels: Predicted output superimposed on top of noise-free output.

IDENTIFICATION OF EXPERIMENTAL PITCH-PLUNGE DATA

Lastly, the identification technique is assessed on experimental wing section data collected in the wind tunnel at the Department of Aerospace Engineering at Texas A&M University by the Aeroelasticity Research Group. The data analyzed for this study does not contain a flap control input but instead had an initial condition associated with plunge displacement. Data with a control input was unavailable for analysis.

The velocity model descriptions given in equation (12) are in terms of a control input and zero initial conditions. For the present study the model was modified to reflect a lack of exogenous input and the presence of an initial condition. Equation (12) is reformulated as equation (14):

$$
\begin{aligned}
\dot{h}(n) &= \theta_1\dot{h}(n-1) + \theta_2 h(n-1) + \theta_3\alpha(n-1) + \theta_4\alpha(n-1)^2 + \theta_5\alpha(n-1)^3 \\
&\quad + \theta_6\alpha(n-1)^4 + \theta_7\alpha(n-1)^5 + \theta_8\dot{\alpha}(n-1) + \theta_9\delta(n) + \theta_{10}e_{\dot{h}}(n-1) + e_{\dot{h}}(n) \\
\dot{\alpha}(n) &= \gamma_1\dot{\alpha}(n-1) + \gamma_2 h(n-1) + \gamma_3\alpha(n-1) + \gamma_4\alpha(n-1)^2 + \gamma_5\alpha(n-1)^3 \\
&\quad + \gamma_6\alpha(n-1)^4 + \gamma_7\alpha(n-1)^5 + \gamma_8\dot{h}(n-1) + \gamma_9 e_{\dot{\alpha}}(n-1) + e_{\dot{\alpha}}(n)
\end{aligned}
\tag{14}
$$

where $\delta(n)$ is the Kronecker impulse function used to represent the onset of a plunge initial condition in discrete-time. Note that this model description can also be modified for use in analysis of data that contains both an initial condition and exogenous input by simply including a Kronecker impulse function in equation (12) or excluding both (time-series analysis) by removing the exogenous input term.

Apparatus

Data was collected on a unique wind tunnel test apparatus at the Department of Aerospace Engineering at Texas A&M University. This 2-ft by 3-ft closed-circuit low-speed wind tunnel allows a wing section to move in two degrees-of-freedom and can translate (plunge) and rotate (pitch). This apparatus allows the study of classical bending-torsion flutter. Structural response of the system is governed by springs attached to cams. Stiffness of the springs and the shape of the cams can be altered to prescribe a wide variety of linear and nonlinear structural responses.

Procedures

The pitch acceleration was measured by a linear accelerometer, which measured accelerations along one axis. The accelerometer was mounted 0.157 m from the rotational axis and orthogonal to the y-direction (forward-aft) when the airfoil was at a zero angle of attack, giving no acceleration in the y-direction. However, a small portion of the plunge acceleration was detected when the airfoil was deflected. The elastic axis was three-tenths of the chord length forward of the midchord.

The free-stream velocity was increased in increments of 2 m/s from 4 to 22 m/s. Aeroelastic responses were recorded for 45 s while the free-stream velocity was held constant. Flutter was observed to be induced at about 13.5 m/s. Pitch and plunge displacements and accelerations of this aeroelastic system were sampled at 525 Hz.

After recording, the experimental data was decimated by a factor of 2, resulting in a final sampling rate of 262.5 Hz. The system was identified using the NARMAX approach, as outlined in the section titled “Analysis of NARMAX Model Parameters,” except that $N = 15{,}600$ points was used for estimation and $N_v = 7800$ points was used for validation.

Results

The results of identifying 10 trials of wing section experiments are presented. Figures 5(a) and 5(b) show a typical pitch-plunge displacement and velocity trial used for this analysis. The data represents pitch and plunge displacement and velocity sequences while the free-stream velocity in the wind tunnel was held constant at 16 m/s. The characteristics of this trial are consistent with those reported in previous work (ref. 33). The lower panels of figures 5(c) and 5(d) display a 5-s slice of the cross-validation (predicted) outputs superimposed on top of the measured outputs for this trial. The predicted outputs matched the measured outputs with over 98 %QF.

Figure 6 shows the cross-validation %QF for each trial. The results show that the predicted outputs, for these parameter estimates, account for a large portion of the variance. For pitch velocity, the range of %QF is from a minimum of 99.73 percent to a maximum of 99.98 percent. For plunge velocity, the range of %QF is from a minimum of 98.09 percent to a maximum of 99.83 percent. From the 10 trials examined for this study, 80 percent of predicted outputs accounted for more than 99 %QF of the measured output for both pitch and plunge velocity. This result indicates that the NARMAX parameters explain the measured data well. Moreover, for every data set the standard deviation (STD) of each model parameter was computed at the 95 percent confidence level. These results showed that the STDs did not contain zero and suggest that the estimated models are accurate. A model parameter whose STD encompasses zero may indicate a spurious model term and, hence, should be reformulated (ref. 34).

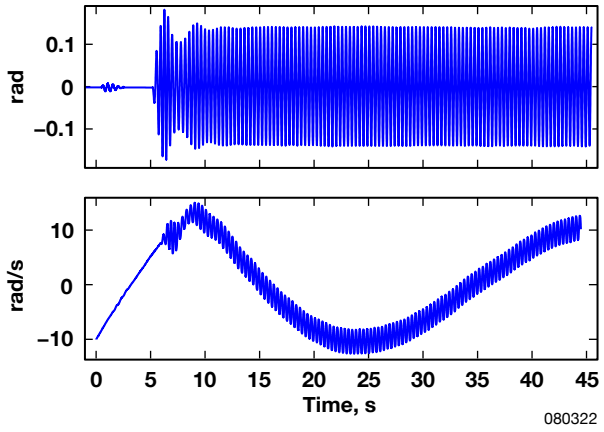

(a). Upper panel: Pitch displacement. Lower panel: Measured pitch velocity.

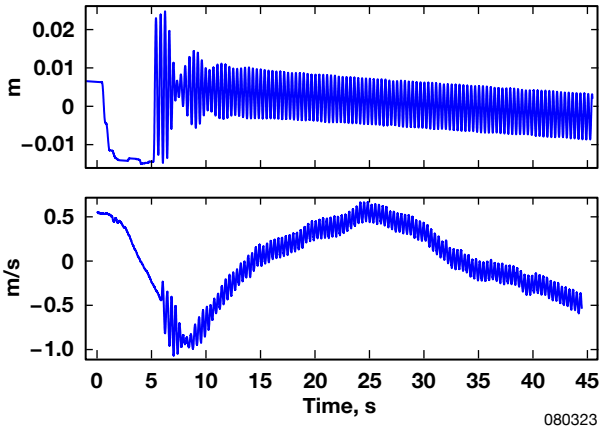

(b). Upper panel: Plunge displacement. Lower panel: Measured plunge velocity.

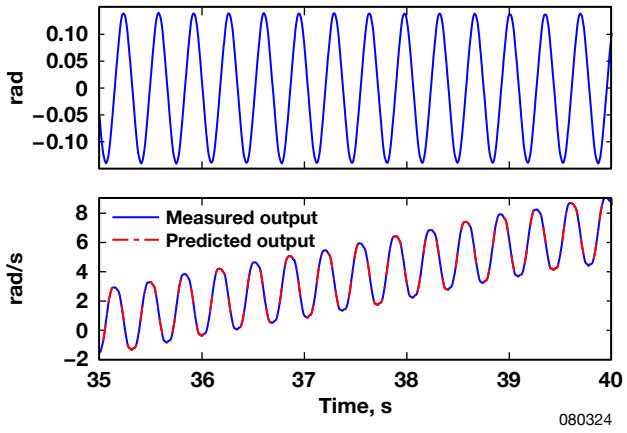

(c). Upper panel: Pitch displacement. Lower panel: Measured and cross-validated pitch velocity, 99.98 %QF.

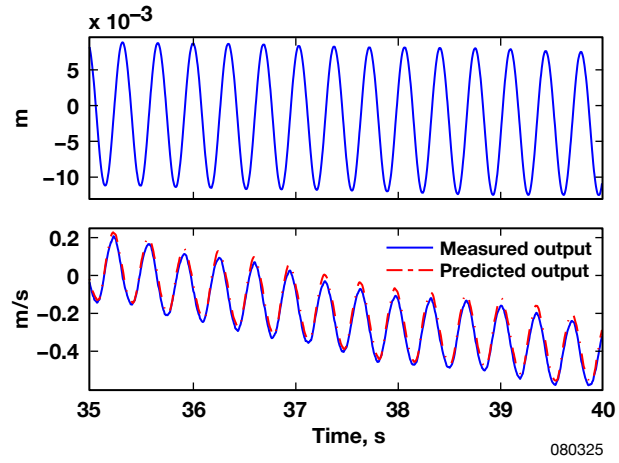

(d). Upper panel: Plunge displacement. Lower panel: Measured and cross-validated plunge velocity, 98.95 %QF.

Figure 5. (a) and (b). Upper and lower panels: Typical recorded pitch and plunge displacement and velocity; (c) and (d). Cross-validation: upper panels: Five-second slice of pitch and plunge displacement; lower panels: Five-second slice of predicted pitch and plunge velocity outputs superimposed on top of measured velocity output for identified NARMAX pitch-plunge velocity models for experimental data set with $N_V = 7800$.

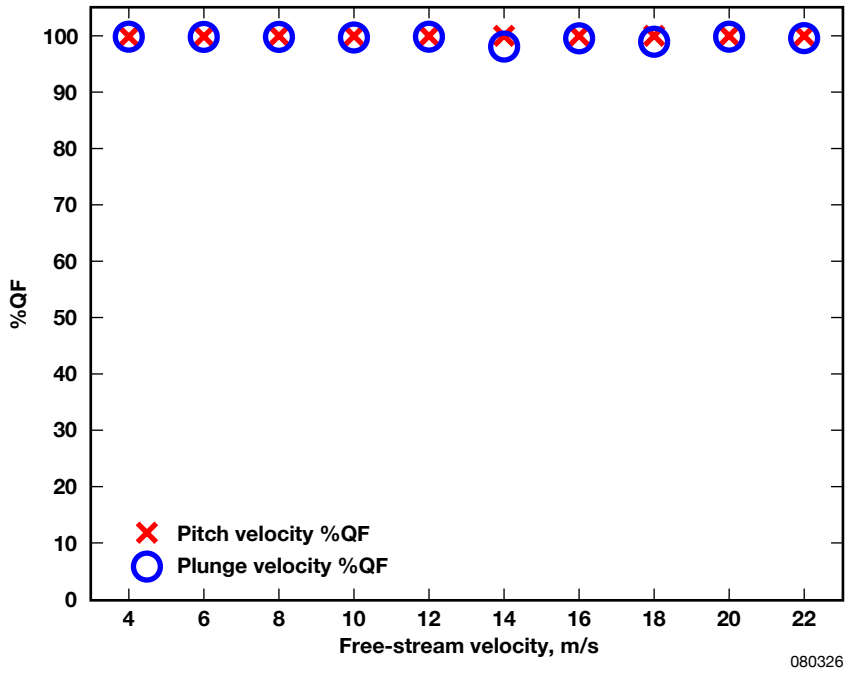

Figure 6. Cross-validation. %QF versus free-stream velocity (experimental trial).

DISCUSSION

NARMAX Representation of Pitch-Plunge Velocity Dynamics

The theoretical results demonstrate that the nonlinear difference equation description for the pitch-plunge models are NARMAX models. Simulation results show that the NARMAX models match the continuous-time response well. These results suggest that parametric nonlinear model forms such as the NARMAX class can be used for modeling aerospace systems.

Nonlinear models have the advantage of covering a wider range of system dynamics than linear models, which could allow for slower envelope expansion. Using nonlinear models to characterize aeroelastic phenomena can provide significant time and cost savings for test and development of aerospace vehicles. Moreover, the discrete nonlinear models of pitch-plunge provide excellent predictions that could be used for control synthesis and statistical studies of NARMAX coefficients and may be of direct relevance for health monitoring of aerostructures.

Discrete-Time Parameter Estimation of Simulated Aeroelastic System

Simulation studies previously described in the section titled “Analysis of NARMAX Model Parameters” showed that, for a NARMAX model representation, the mean of Monte Carlo estimates for NARMAX parameters matched the theoretical values well for all SNR

levels. However, estimates of some parameters (e.g., γ_{10}) did not correspond well to theoretically computed values. As previously stated, lagged-error terms are difficult to identify accurately. Error terms represent a stochastic process that cannot be measured. This stochastic process is approximated by a deterministic signal of prediction errors that is only an (poor) estimate of the noise (refs. 22 and 28).

Identification of Experimental Aeroelastic Data

High %QF cross-validation fits obtained for parameter estimates using NARMAX identification methods (fig. 6) show that the identified parameters explain the experimental data well. Using %QF alone as an indicator of model goodness may lead to incorrect interpretations of model validity. However, in many cases for nonlinear models, %QF may be the only indicator that is readily available.

A model validation technique for nonlinear systems, using higher order correlations, was developed by Billings and Voon (refs. 35 and 36). Korenberg and Hunter (ref. 37) showed that this model validation technique fails for simple cases. Therefore, this approach was not implemented in favor of using the %QF alone as an indicator of model goodness.

When studying aeroelastic systems, assuming that the exact model order and structure are well-known a priori may not be practical. In aerospace systems analysis, one of the main objectives is not only to estimate system parameters but also to gain insight into the structure of the underlying system. Investigation in a future study would be worthwhile to determine the result of allowing NARMAX structure detection methods (refs. 34 and 38–40) to analyze the data to find the best structure from the data set. This may then indicate deficiencies in the analytical model and could lead to improved modeling strategies.

CONCLUSIONS

Theoretical results demonstrate that the nonlinear difference equation description for the pitch-plunge model is a NARMAX model. Simulation results show that the NARMAX model matches the continuous-time response well. Moreover, this report contributes to the understanding of the use of parametric identification techniques for modeling of nonlinear aerospace systems. The main point here is that the NARMAX form is clearly amenable to the study of a wide range of aerospace systems and could be computationally efficient. NARMAX modeling and identification techniques should be examined further especially in the case of severe nonlinear behavior.

REFERENCES

1. Lee, B. H. K., S. J. Price, and Y. S. Wong, “Nonlinear aeroelastic analysis of airfoils: bifurcation and chaos,” *Progress in Aerospace Sciences*, vol. 35, no. 3, pp. 205–334, Elsevier, Amsterdam, 1999.

2. Bunton, Robert W., and Charles M. Denegri, Jr., “Limit Cycle Oscillation Characteristics of Fighter Aircraft,” *Journal of Aircraft*, vol. 37, no. 5, pp. 916–918, AIAA, New York, 2000.

3. Chen, P. C., D. Sarhaddi, and D. D. Liu, “Limit-Cycle-Oscillation Studies of a Fighter with External Stores,” AIAA-1998-1727, AIAA, New York, 1998.

4. Denegri, Charles M., Jr., “Limit Cycle Oscillation Flight Test Results of a Fighter with External Stores,” *Journal of Aircraft*, vol. 37, no. 5, pp. 761–769, AIAA, New York, 2000.

5. Greblicki, Wlodzimierz, and Miroslaw Pawlak, “Nonparametric identification of a cascade nonlinear time series system,” *Signal Processing*, vol. 22, issue 1, pp. 61–75, Elsevier, Amsterdam, 1991.

6. Kosut, Robert L., Ming K. Lau, and Stephen P. Boyd, “Set-Membership Identification of Systems with Parametric and Nonparametric Uncertainty,” *IEEE Transactions on Automatic Control*, vol. 37, no. 7, pp. 929–941, IEEE, New York, 1992.

7. Masri, S. F., and T. K. Caughey, “A Nonparametric Identification Technique for Nonlinear Dynamic Problems,” *Journal of Applied Mechanics*, vol. 46, pp. 433–447, ASME, New York, 1979.

8. Lind, Rick, Richard J. Prazenica, and Martin J. Brenner, “Estimating Nonlinearity Using Volterra Kernels in Feedback with Linear Models,” *Nonlinear Dynamics*, vol. 39, nos. 1–2, pp. 3–23, Springer, The Netherlands, 2005.

9. Leontaritis, I. J., and S. A. Billings, “Input-output parametric models for non-linear systems Part I: deterministic non-linear systems,” *International Journal of Control*, vol. 41, no. 2, pp. 303–328, Taylor & Francis, London, 1985.

10. Leontaritis, I. J., and S. A. Billings, “Input-output parametric models for non-linear systems Part II: stochastic non-linear systems,” *International Journal of Control*, vol. 41, no. 2, pp. 329–344, Taylor & Francis, London, 1985.

11. Billings, S. A., and S. Chen, “Extended model set, global data and threshold model identification of severely non-linear systems,” *International Journal of Control*, vol. 50, no. 5, pp. 1897–1923, Taylor & Francis, London, 1989.

12. Chen, S., and S. A. Billings, “Representations of non-linear systems: the NARMAX model,” *International Journal of Control*, vol. 49, no. 3, pp. 1013–1032, Taylor & Francis, London, 1989.

13. Chen, S., S. A. Billings, C. F. N. Cowan, and P. M. Grant, “Practical identification of NARMAX models using radial basis functions,” *International Journal of Control*, vol. 52, no. 6, pp. 1327–1350, Taylor & Francis, London, 1990.

14. Kukreja, S. L., H. L. Galiana, and R. E. Kearney, “NARMAX representation and identification of ankle dynamics,” *IEEE Transactions on Biomedical Engineering*, vol. 50, issue 1, pp. 70–81, IEEE, New York, 2003.

15. O’Neil, Todd, and Thomas W. Strganac, “Nonlinear Aeroelastic Response–Analyses and Experiments,” AIAA-1996-0014, AIAA, New York, 1996.

16. O’Neil, Todd, Heather Gilliatt, and Thomas W. Strganac, “Investigations of Aeroelastic Response for a System with Continuous Structural Nonlinearities,” AIAA-1996-1390, AIAA, New York, 1996.

17. Dowell, Earl H., “Nonlinear Aeroelasticity,” AIAA-1990-1031, *AIAA/ASME/ASCE/AHS/ASC 31st Structures, Structural Dynamics, and Materials Conference, Part 3, A Collection of Technical Papers*, pp. 1497–1509, AIAA, New York, 1990.

18. Tang, D. M., and E. H. Dowell, “Flutter and Stall Response of a Helicopter Blade with Structural Nonlinearity,” *Journal of Aircraft*, vol. 29, no. 5, pp. 953–960, AIAA, New York, 1992.

19. Yang, Z. C., and L. C. Zhao, “Analysis of Limit Cycle Flutter of an Airfoil in Incompressible Flow,” *Journal of Sound and Vibration*, vol. 123, issue 1, pp. 1–13, Elsevier, Amsterdam, 1988.

20. Zhao, L. C., and Z. C. Yang, “Chaotic Motions of an Airfoil with Non-linear Stiffness in Incompressible Flow,” *Journal of Sound and Vibration*, vol. 138, issue 2, pp. 245–254, Elsevier, Amsterdam, 1990.

21. Franklin, Gene F., J. David Powell, and Abbas Emami-Naeini, *Feedback Control of Dynamic Systems*, 4th ed., Prentice Hall, Upper Saddle River, New Jersey, 2002.

22. Ljung, Lennart, *System Identification: Theory for the User*, 2nd ed., Prentice Hall, Upper Saddle River, New Jersey, 1999.

23. Åström, Karl J., and Björn Wittenmark, *Computer-Controlled Systems: Theory and Design*, 3rd ed., Prentice Hall, Upper Saddle River, New Jersey, 1996.

24. Panuska, V., “A Stochastic Approximation Method for Identification of Linear Systems Using Adaptive Filtering,” *Proceedings of the 1968 Joint Automatic Control Conference of the American Automatic Control Council*, pp. 1014–1021, IEEE, New York, 1968.

25. Panuska, V., "An adaptive recursive-least-squares identification algorithm," *Proceedings of the 1969 IEEE Conference on Decision & Control including the 8th Symposium on Adaptive Processes*, vol. 8, pt. 1, p. 65, IEEE, New York, 1969.

26. Young, Peter C., "The Use of Linear Regression and Related Procedures for the Identification of Dynamic Processes," *IEEE Proceedings of Seventh Symposium on Adaptive Processes*, pp. 5-c-1–5-c-5, IEEE, New York, 1968.

27. Billings, S. A., and W. S. F. Voon, "Least squares parameter estimation algorithms for non-linear systems," *International Journal of Systems Science*, vol. 15, no. 6, pp. 601–615, Taylor & Francis, London, 1984.

28. Goodwin, Graham C., and Robert L. Payne, *Dynamic System Identification: Experiment Design and Data Analysis*, *Mathematics in Science and Engineering* book series, vol. 136, Academic Press, New York, 1977.

29. Walter, Éric, and Luc Pronzato, *Identification of Parametric Models from Experimental Data*, Springer, New York, 1997.

30. Söderström, Torsten, and Petre Stoica, *System Identification*, Prentice Hall, New York, 1989.

31. Stoica, Petre, and Torsten Söderström, "Asymptotic behaviour of some bootstrap estimators," *International Journal of Control*, vol. 33, no. 3, pp. 433–454, Taylor & Francis, London, 1981.

32. Shao, Jun, "Linear Model Selection by Cross-Validation," *Journal of the American Statistical Association*, vol. 88, no. 422, pp. 486–494, American Statistical Association, New York, 1993.

33. Kurdila, Andrew J., Richard J. Prazenica, Othon Rediniotis, and Thomas Strganac, "Multiresolution Methods for Reduced-Order Models for Dynamical Systems," *Journal of Guidance, Control, and Dynamics*, vol. 24, no. 2, pp. 193–200, AIAA, New York, 2001.

34. Kukreja, Sunil L., Henrietta L. Galiana, and Robert E. Kearney, "A bootstrap method for structure detection of NARMAX models," *International Journal of Control*, vol. 77, no. 2, pp. 132–143, Taylor & Francis, London, 2004.

35. Billings, S. A., and W. S. F. Voon, "Structure detection and model validity tests in the identification of nonlinear systems," *IEE Proceedings, Part D–Control Theory and Applications*, vol. 130, no. 4, pp. 193–199, IEE, Stevanage, UK, 1983.

36. Billings, S. A., and W. S. F. Voon, "Correlation based model validity tests for non-linear models," *International Journal of Control*, vol. 44, no. 1, pp. 235–244, Taylor & Francis, London, 1986.

37. Korenberg, Michael J., and Ian W. Hunter, “The Identification of Nonlinear Biological Systems: Wiener Kernel Approaches,” *Annals of Biomedical Engineering*, vol. 18, pp. 629–654, Springer, The Netherlands, 1990.

38. Korenberg, Michael, “Orthogonal Identification of Nonlinear Difference Equation Models,” *Conference Proceedings of the 28th Midwest Symposium on Circuits and Systems*, vol. 1, pp. 90–95, University of Louisville, 1985.

39. Korenberg, M., S. A. Billings, Y. P. Liu, and P. J. McIlroy, “Orthogonal parameter estimation algorithm for non-linear stochastic systems,” *International Journal of Control*, vol. 48, no. 1, pp. 193–210, Taylor & Francis, London, 1988.

40. Kukreja, Sunil L., Robert E. Kearney, and Henrietta L. Galiana, “A Bootstrap Method for NARMAX Model Order Selection,” *Modelling and Control in Biomedical Systems 2000*, a Proceedings volume from the 4th IFAC Symposium, pp. 329–332, Pergamon, New York, 2000.

REPORT DOCUMENTATION PAGE

Form Approved
OMB No. 0704-0188

1. REPORT DATE *(DD-MM-YYYY)*	2. REPORT TYPE	3. DATES COVERED *(From - To)*
01-11-2008	Technical Memorandum	

4. TITLE AND SUBTITLE
Nonlinear System Identification for Aeroelastic Systems with Application to Experimental Data

5a. CONTRACT NUMBER

5b. GRANT NUMBER

5c. PROGRAM ELEMENT NUMBER

6. AUTHOR(S)
Dr. Sunil L. Kukreja

5d. PROJECT NUMBER

5e. TASK NUMBER

5f. WORK UNIT NUMBER

7. PERFORMING ORGANIZATION NAME(S) AND ADDRESS(ES)
NASA Dryden Flight Research Center
P.O. Box 273
Edwards, California 93523-0273

8. PERFORMING ORGANIZATION REPORT NUMBER
H-2887

9. SPONSORING/MONITORING AGENCY NAME(S) AND ADDRESS(ES)
National Aeronautics and Space Administration
Washington, DC 20546-0001

10. SPONSORING/MONITOR'S ACRONYM(S)
NASA

11. SPONSORING/MONITORING REPORT NUMBER
NASA/TM-2008-214641

12. DISTRIBUTION/AVAILABILITY STATEMENT
Unclassified--Unlimited
Subject Category 31 Availability: NASA CASI (301) 621-0390 Distribution: Standard

13. SUPPLEMENTARY NOTES
Kukreja, NASA Dryden Flight Research Center. Also presented as AIAA-2008-7392 at the AIAA Guidance, Navigation and Control Conference and Exhibit, Honolulu, Hawaii, August 18-21, 2008. An electronic version can be found at http://dtrs.dfrc.nasa.gov or http://ntrs.nasa.gov/search.jsp.

14. ABSTRACT
Representation and identification of a nonlinear aeroelastic pitch-plunge system as a model of the Nonlinear AutoRegressive, Moving Average eXogenous (NARMAX) class is considered. A nonlinear difference equation describing this aircraft model is derived theoretically and shown to be of the NARMAX form. Identification methods for NARMAX models are applied to aeroelastic dynamics and its properties demonstrated via continuous-time simulations of experimental conditions. Simulation results show that (1) the outputs of the NARMAX model closely match those generated using continuous-time methods, and (2) NARMAX identification methods applied to aeroelastic dynamics provide accurate discrete-time parameter estimates. Application of NARMAX identification to experimental pitch-plunge dynamics data gives a high percent fit for cross-validated data.

15. SUBJECT TERMS
Aeroelasticity, Modeling, NARMAX, Nonlinear system identification, Pitch-plunge model

16. SECURITY CLASSIFICATION OF:			17. LIMITATION OF ABSTRACT	18. NUMBER OF PAGES	19b. NAME OF RESPONSIBLE PERSON
a. REPORT	b. ABSTRACT	c. THIS PAGE			STI Help Desk (email: help@sti.nasa.gov)
					19b. TELEPHONE NUMBER *(Include area code)*
U	U	U	UU	31	(301) 621-0390